Leakage Mechanism of Ferroelectric $Al_{0.7}Sc_{0.3}N$ Ultra-thin Film

Li Chen
Institute of Microelectronics
*Agency for Science, Technology and Research (A*STAR)*
Singapore
chen_li@ime.a-star.edu.sg

Zichu Wang
Institute of Microelectronics
*Agency for Science, Technology and Research (A*STAR)*
Singapore
ZichuW.GE2122@tum-asia.edu.sg

Chen Liu
Institute of Microelectronics
*Agency for Science, Technology and Research (A*STAR)*
Singapore
liu_chen@ime.a-star.edu.sg

Minghua Li
Institute of Microelectronics
*Agency for Science, Technology and Research (A*STAR)*
Singapore
li_minghua@ime.a-star.edu.sg

Wendong Song
Institute of Microelectronics
*Agency for Science, Technology and Research (A*STAR)*
Singapore
song_wen_dong@ime.a-star.edu.sg

Weijie Wang
Institute of Microelectronics
*Agency for Science, Technology and Research (A*STAR)*
Singapore
wang_weijie@ime.a-star.edu.sg

Binni Varghese
Institute of Microelectronics
*Agency for Science, Technology and Research (A*STAR)*
Singapore
binni_varghese@ime.a-star.edu.sg

Hock Koon Lee
Institute of Microelectronics
*Agency for Science, Technology and Research (A*STAR)*
Singapore
lee_hock_koon@ime.a-star.edu.sg

Huamao Lin
Institute of Microelectronics
*Agency for Science, Technology and Research (A*STAR)*
Singapore
lin_huamao@ime.a-star.edu.sg

Yao Zhu
Institute of Microelectronics
*Agency for Science, Technology and Research (A*STAR)*
Singapore
zhuya@ime.a-star.edu.sg

***Abstract*—The remarkable ferroelectric properties discovered in scandium-doped aluminum nitride (AlScN) has generated tremendous research interest. Preliminary investigations indicate that the $Al_{1-x}Sc_xN$ could encounter substantial leakage current when scales down the thickness, potentially limiting its practical implementation on memory applications. In this work, taking the 50 nm and 30 nm ultra-thin $Al_{0.7}Sc_{0.3}N$ films as vehicle, we systematically analyzed the key factor contributing the leakage current *via* Poole-Frenkel (P-F) emission fitting. The result shows that it is the defect concentration leading to the large leakage instead of the trap energy level (Φ_T).**

Keywords—Ferroelectric $Al_{0.7}Sc_{0.3}N$, leakage current, P-F emission, defect, trap energy level

I. Introduction

The utilization of scandium-doped aluminum nitride (AlScN) as a piezoelectric material has triggered significant research interest over the past few years. It has been extensively demonstrated for applications in MEMS resonators, filters, and transducers. [1-6]. In more recent developments, the demonstration of ferroelectricity in AlScN has unveiled its tremendous potential for ferroelectric memory applications [7]. AlScN surpasses other conventional ferroelectric materials in several aspects, including possessing a large remnant polarization (P_r) exceeding 100 µC/cm^2, the ability to scale down to sub-10 nm dimensions, and is compatible with CMOS-BEOL processes [8-10]. Inspiringly, researchers have achieved successful demonstrations of various memory devices utilizing AlScN. These include the developments of ferroelectric field transistor (FeFET) by integrating AlScN gate stack with a two-dimensional channel material [11], as well as the creation of an array of ferroelectric diodes for in-memory computing [12]. Nevertheless, initial studies have observed a significant increment of leakage current in AlScN when reduces the thickness of the film, which may impede its practical implementation on memory applications [10]. Previous works have identified that the dominant conduction mechanism of AlScN is the P-F emission [13]. However, the key contributor resulting in the increasing leakage current is still unknow yet. In this work, we systematically investigated the dominant factor leading to the rising leakage by comparing the leakage current of the AlScN film with thickness of 50 nm and 30nm. Leveraging on the P-F emission fitting, it is found that the defect concentration is the main factor causing the higher leakage current rather than the trap energy level when the thickness reduces.

II. Experimental

Fig. 1 illustrates the structure of the metal-ferroelectric-metal (MFM) capacitors array based on $Al_{0.7}Sc_{0.3}N$. To begin with, a layer of molybdenum with a thickness of 200 nm is sputtered onto the 8-inch silicon substrate, acting as the bottom electrode. Then, 50/30 nm $Al_{0.7}Sc_{0.3}N$ thin film is deposited by alloy-target sputtering. A layer of Mo with a thickness of 100 nm is subsequently deposited without vacuum break and serves as the top electrode. Finally, top circular electrodes with a radius of 50 μm are patterned and

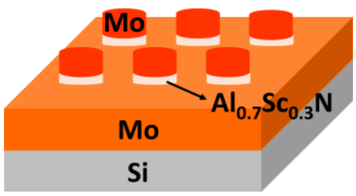

Fig. 1. Schematic of the $Al_{0.7}Sc_{0.3}N$-based capacitors array.

created *via* dry etching. The growth process of the $Al_{0.7}Sc_{0.3}N$ films with different thicknesses follows a consistent recipe, and the modulation of thickness is achieved by adjusting the growth time.

The transient current of the MFM capacitor was measured by applying triangle pulses with a frequency of 10 kHz using Radiant ferroelectric test system and the DC leakage current of the device was characterized by Keysight B1500A semiconduction device parameter analyzer.

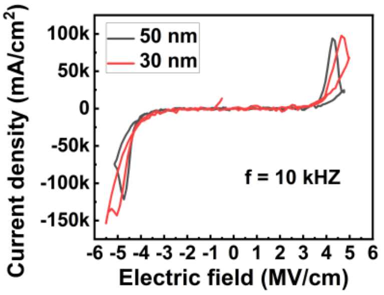

Fig. 2. Dynamic *J-E* curves of the devices with film thickness of 50 nm and 30nm, respectively.

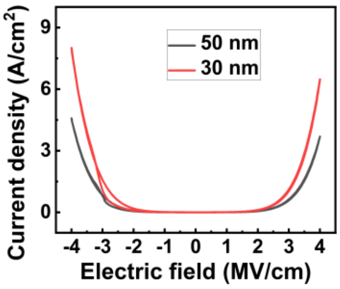

Fig. 3. DC *J-E* curves of the devices with film thickness of 50 nm and 30nm, respectively.

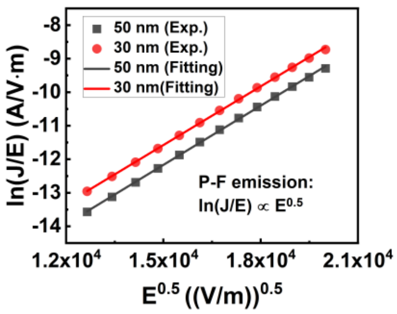

Fig. 4. Fitting of experimental $\ln(J/E)$-$E^{0.5}$ results to the P-F model of devices with film thickness of 50 nm and 30nm.

III. Results and Discussion

Fig. 2 shows the representative *J-E* loops of the as-fabricated $Al_{0.7}Sc_{0.3}N$-based capacitor with film thickness of 50 nm and 30 nm, respectively. Ferroelectric-induced switching current is observed in both devices. In the meanwhile, it is found that the device with film thickness of 30 nm obtains a larger coercive field (E_c), which may result from the more compressive stress in the thinner film. Thus, to enable AlScN for practical implementation, strain engineering is required to reduce the E_c to reduce the operating voltage. **Fig. 3** depicts the typical DC *J-E* curves of the devices with different thicknesses. The leakage current is at mA/cm^2 level

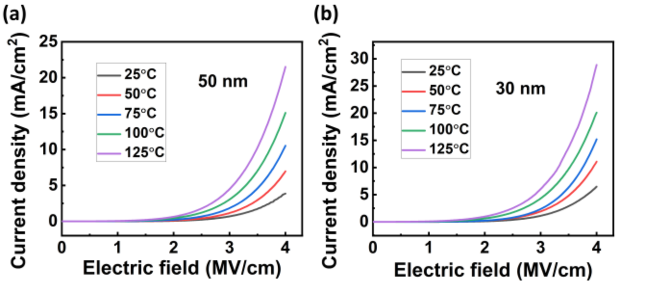

Fig. 5. Temperature-dependent DC *J-E* curves of the devices with film thickness of 50 nm and 30 nm, respectively.

at $E = \pm 4$ MV/cm, and the leakage current of the device with

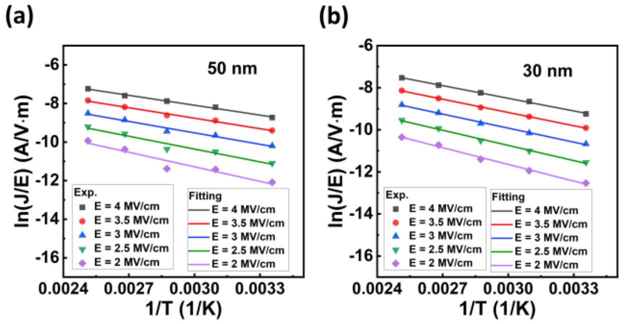

Fig. 6. Fitting of experimental $\ln(J/E)$-$1/T$ results to the P-F model of devices with film thickness of 50 nm and 30nm, respectively.

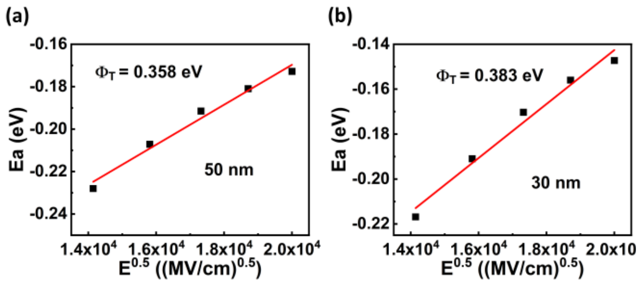

Fig. 7. Fitting of experimental E_a-$E^{0.5}$ results to the P-F model of devices with film thickness of 50 nm and 30nm, respectively.

film thickness of 30 nm is twice as large as that of the device with film thickness of 50 nm. It has been reported that the conduction mechanism of the AlScN is P-F emission [13]. However, the primary contributor to the large leakage is still under debate. To explore the key factor that contributes to the large leakage, the systematic P-F emission fittings are then performed. The P-F emission can be expressed as:

$$J = q\mu n_0 E \exp[-\frac{q\phi_T - \sqrt{q^3 E/\pi\varepsilon_0\varepsilon_r}}{kT}], (1)$$

where μ is the carrier mobility, q is the elementary charge, $q\phi_T (= \Phi_T)$ is the trap energy level, n_0 is the density of states in the conduction band, k is the Boltzmann constant, T is the absolute temperature, ε_0 is the vacuum permittivity, and ε_r is the optical dielectric constant. The major factors in the P-F emission are the trap energy level and the concentration of traps. Generally, both a higher defect concentration and a lower trap energy level will cause a higher leakage current. **Fig. 4** plots $\ln(J/E)$-$E^{0.5}$ curves of the devices with different thicknesses, showing good linearity. This indicates both the devices follows the dependency of the P-F emission. After the confirmation of conduction mechanism, we then performed the temperature-dependent DC leakage test to extract trap energy level. The DC *J-E* curves of the devices under different temperature are plotted in **Fig. 5**. The leakage current increases monotonously with the increasing temperature. The ln(*J-E*) - 1/*T* curves exhibit clear linearity for both devices as shown in **Fig. 6**, and the slopes are extracted to obtain the Φ_T. **Fig. 7** depicts E_a-$E^{0.5}$ curves for both devices, where $E_a = -q\phi_T + \sqrt{q^3E/\pi\varepsilon_0\varepsilon_r}$. The Φ_T values are extracted from the interception of the linear fitting curve and y-axis. It is found that the thinner film has a larger trap energy level (~ 0.383 eV) (**Fig. 7(b)**) compared with that of the thicker film (~0.358 eV) (**Fig. 7(a)**), indicating that the trap energy level is not the root for causing a higher leakage current when scales the thickness. On the contrary, the trap density is the key factor.

IV. CONCLUSIONS

In this work, we compared the leakage current of the AlScN film with thicknesses of 50 nm and 30 nm, respectively, and did systematic P-F emission fitting to understand the main factor contributes to the higher leakage current when scales down the dimension. It is observed that the concentration of the traps instead of trap energy level is the main contributor to the increasing leakage current.

ACKNOWLEDGMENT

This work was supported by the Science and Engineering Research Council of A*STAR (Agency for Science, Technology and Research) Singapore, under Grant No. A20G9b0135.

REFERENCES

[1] M. Akiyama, T. Kamohara, K. Kano, A. Teshigahara, Y. Takeuchi and N. Kawahara, "Enhancement of piezoelectric response in scandium aluminum nitride alloy thin films prepared by dual reactive cosputtering," *Adv. Mater.,* 2009, 21, pp. 593–596.

[2] Y. Zhu, N. Wang, G. L. Chua, C. Sun, N. Singh, and Y. Gu, "ScAlN-based LCAT mode resonators above 2 GHz with high FOM and reduced fabrication complexity," *IEEE Electron Device Lett.,* 2017, 38, pp,1481-1484.

[3] N. Wang, Y. Zhu, G. L. Chua, B, Chen, S. Merugu, N. Singh, and Y. Gu, "Over 10% of k_{eff}^2 demonstrated by 2-GHz spurious mode-free $Sc_{0.12}Al_{0.88}N$ laterally coupled alternating thickness mode resonators," IEEE Electron Device Lett., 2019, 40, pp. 957-960.

[4] N. Wang, Y. Zhu, B, Chen, and Y. Zhang, "Over 12% of coupling coefficient demonstrated by 3GHz $Sc_{0.12}Al_{0.88}N$ based laterally coupled alternatin thickness (LCAT) mode resonators laterally coupled alternating thickness mode resonators," 2019 *IEEE Int, Ultrasonic Symp. (IUS)*, 2019. pp. 1971-1973, doi: 10.1109/ULTSYM.2019.8926087.

[5] Y. Zhang, X. Wnag, C. Liu, E. Y. Z. Woo, W. Yang, Q. Zhang, H. Lin, D. Yan, R. M. Kumarasamy, B. Chen, N. Wang, Y. Zhu, "3D Monolithic Integration of ScAlN-based GHz MEMS Acoustic Filters on 200mm RFSOI Wafer," *2022 International Electron Devices Meeting (IEDM)*, , 2022, pp. 16.2.1-16.2.4, doi: 10.1109/IEDM45625.2022.10019557.

[6] L. Chen, C. Liu, M. Li, W. Song, W. Wang, Z. Wang, N. Wang, Y. Zhu, "Scanduim-doped aluminum nitride for acoustic wave resonators, filters, and ferroelectric memory applications," *ACS Appl. Electron. Mater.*, 2023, 5, 612-622

[7] S. Fichtner, N. Wolff, F. Lofink, L. Kienle, and B. Wagner, "AlScN: A III-V semiconductor based ferroelectric," *J. Appl. Phys.*, 2019, *125*, p.114103.

[8] L. Chen, C. Liu, M. Li, W. Song, W. Wang, Z. Chen, S. Samanta, H. K. Lee, Y. Zhu, "Bipolar and Unipolar Cycling Behavior in Ferroelectric Scandium-doped Aluminum Nitride," *2022 IEEE International Symposium on Applications of Ferroelectrics (ISAF)*, 2022, pp. 1-3, doi: 10.1109/ISAF51494.2022.9870042.

[9] G. Schönweger, N. Wolff, M. R. Islam, M. Gremmel, A. Petraru, L. Kienle, H. Kohlstedt, S. Fichtner, "In-Grain Ferroelectric Switching in Sub-5 nm Thin $Al_{0.74}Sc_{0.26}N$ Films at 1 V," *Adv. Sci.*, 2023, p.2302296.

[10] J. X. Zheng, M. M. A. Fiagbenu, G. Esteves, P. Musavigharavi, A. Gunda, D. Jariwala, E. A. Stach, R. H. Olsson, "Ferroelectric behavior of sputter deposited $Al_{0.72}Sc_{0.28}N$ approaching 5 nm thickness," *Appl. Phys. Lett.*, 2023, 122, 222901.

[11] X. Liu, J. Ting, Y. He, M. M. A. Fiagbenu, J. Zheng, D. Wang, J. Frost, P. Musavigharavi, G. Esteves, K. Kisslinger, S. B. Anantharaman, E. A. Stach, R. H. Olsson, D. Jariwala, "Reconfigurable compute-in-memory on field-programmable ferroelectric diodes," *Nano Lett.*, *2022, 22*, pp.7690-7698.

[12] K. H. Kim, S. Oh, M. M. A. Fiagbenu, J. Zheng, P. Musavigharavi, P. Kumar, N. Trainor, A. Aljarb, Y. Wan, H. M. Kim, K. Katti, S. Song, G. Kim, Z. Tang, J. Fu, M. Hakami, V. Tung, J. M. Redwing, A. Stach, R. H. Olsson, D. Jariwala, "Scalable CMOS back-end-of-line-compatible AlScN/two-dimensional channel ferroelectric field-effect transistors," *Nature Nanotechnol.*, 2023, pp.1-7.

[13] C. Liu, Q. Wang, W. Yang, T. Cao, L. Chen, M. Li, F. Liu, D.K. Loke, J. Kang, and Y. Zhu, "Multiscale modeling of $Al_{0.7}Sc_{0.3}N$-based FeRAM: the steep switching, leakage and selector-free array," 2021 *IEEE International Electron Devices Meeting (IEDM),* 2021, pp. 8-1

.